INVESTIGATING THE INFLUENCE OF THE 3D MUSCLE REPRESENTATION WITH HYBRID ACTIVE PROPERTIES IN THE ANSYS HANS HUMAN BODY MODEL FOR VEHICLE SAFETY APPLICATIONS

Mukund Thirugnanasambanthar
Alexander Gromer
Ansys, Part of Synopsys
Germany

Michael Ditthardt
Christian Kleinbach
Mercedes-Benz AG
Germany

Oleksandr V. Martynenko
Syn Schmitt
Institute for Modelling and Simulation of Biomechanical Systems,
University of Stuttgart
Germany

Paper Number 26-0163

ABSTRACT

Modern finite element Human Body Models (HBM) aim to replicate real human anatomy through detailed modelling of internal organs, the skeletal system, and retaining three-dimensional (3D) muscle shapes. However, when they are used to simulate muscle-driven actions, the question of accurately representing the function of the muscular system arises. Traditionally, active muscle modelling for HBMs in automotive safety employs discrete one-dimensional (1D) beam elements with Hill-type material models, using a controller with different motor control strategies. Though effective for simplified HBMs, this method shows limitations in detailed, separated-tissue models. This work addresses these issues in active HBMs (AHBMs) with detailed 3D muscle structure, focusing on kinematics and injury risk.

The authors propose a hybrid muscle model, that combines 1D finite elements, using an open-source modified Extended Hill-type Muscle Model (EHTM), with a passive 3D matrix featuring a hyperelastic material. The validated model is integrated into the Ansys Hans HBM to test the applicability in a pedestrian impact load case and examine the kinematics associated with it.

The results showcase that the hybrid muscle model coupled through shared nodes produced a stable response compared to the traditional, standalone 1D beam approach. The outcomes show a considerable influence of the activated hybrid muscles, reducing the risks of extremity injury and affecting the kinematics of the HBM. This approach leverages 3D muscle structure and eliminates constraints arising from 1D Hill-type elements, such as muscle routing.

The major limitation to be addressed in future work is to develop efficient whole-body muscle control strategies, as modelling complex movement sequences requires costly optimization of numerous muscle activations for accurate, fast FE HBM simulations. The suggested method enhances existing computational HBMs with an accurate physiological muscle structure, enabling the modelling of active and reactive human responses and offering the potential to improve protection for vulnerable road users and occupants.

Keywords: Active Human Body Model, Finite Element Method, Hill-Type Muscle Model, 3D Muscle Geometry, Hybrid Muscle Modelling

INTRODUCTION

Current advancements in FE HBMs have enhanced anatomical representation and biofidelity by enabling detailed modeling of internal organs and the skeletal system, clear demarcation of soft tissues, and preservation of accurate three-dimensional (3D) muscle geometry. For example, the recent versions of the Total Human Model for Safety (THUMS) [1], Global Human Body Models Consortium (GHBMC) [2], and Ansys Hans [3] human body models illustrate these improvements by incorporating comprehensive representations of thoracic, abdominal, and musculoskeletal structures, thereby achieving high levels of anatomical accuracy. However, despite all advancements, a significant challenge remains for these models in simulating active muscle-driven actions utilizing the whole 3D volume of complex skeletal muscle tissue architecture [4]. It happens because HBMs are commonly developed using static image data and are validated against cadaver data. This approach often fails to accurately represent real-world occupants and pedestrians, whose muscles remain active during pre-crash events, such as emergency braking or evasive maneuvers, as well as following low-speed impacts.

To address these issues, AHBMs were developed to predict variability in human response by modeling active human motion utilizing different muscle activation levels and motor control strategies [5], by this means offering a more realistic way to simulate an accident. Typically, they employ computationally effective one-dimensional discrete beam or truss elements with a Hill-type material model [6] governed by a controller code that generates physiologically plausible activation signals. Such an approach provides satisfactory results in AHBMs with simplified homogeneous material structures but has significant limitations when applied to detailed designs with separated tissue, significantly reducing the complexity of heterogeneous structures and functions to a few lumped parameters. Therefore, the authors suggest adopting the 3D hybrid active muscle model instead, which accurately represents the material complexity of skeletal muscle tissue while ensuring computational feasibility. This hybrid modeling approach typically integrates three-dimensional continuum elements with one-dimensional Hill-type elements into one combined structure to achieve a balance between biofidelity and computational efficiency.

The current contribution addresses the aspects of such a 3D Hybrid active muscle model application that moves beyond the limitations of passive HBMs to provide a biomechanically realistic evaluation of how active human responses affect the accuracy of kinematic predictions and injury risk assessments in vehicular crashes, for both pedestrians and occupants.

METHODS

State of the Art One-Dimensional Muscle Model

Active muscle modeling in HBMs has typically been performed using one-dimensional discrete truss or beam elements along with Hill-type material models, which employ springs and dampers arranged in various configurations to simulate the skeletal muscle response [6]. The current material library of LS-DYNA includes several one-dimensional Hill-type muscle materials, such as **`*MAT_SPRING_MUSCLE`** (**`*MAT_S15`**) and **`*MAT_MUSCLE`** (**`*MAT_156`**) [7]. The **`*MAT_S15`** consists of a Contractile Element (CE) connected in series with a Serial Elastic Element (SEE) and a Parallel Elastic Element (PEE) in parallel (see Figure 1 a)). The total force exerted by the muscle is calculated as the sum of the forces from the CE and the PEE. The SEE is modelled to represent the tendon and can be turned on or off using a flag in the material card. The **`*MAT_156`** serves as an extension of **`*MAT_S15`** by incorporating a parallel damping element to enhance stability (see Figure 1 b)). Although these models are commonly used, they rely on empirical relationships that are not specific to muscles and are not derived directly from anatomical textbooks. The input parameters in the LS-DYNA material cards, such as relative length, shortening velocity, and dimensionless parameters, like tensile stress as a function of stretch ratio and strain rate, are often difficult to obtain from the literature, as they require curves tuning using optimization methods to achieve specific objectives.

For instance, the force generated by the contractile element F_{CE} for **`*MAT_S15`** is expressed as follows:

$$F_{CE} = a(t) \cdot F_{max} \cdot f_{TL}(L) \cdot f_{TV}(V) \qquad \text{(Equation 1)}$$

where $a(t)$ represents the load curve for muscle activation, F_{max} is the maximum isometric force of the muscle, $f_{TL}(L)$ denotes the tension-length relationship and $f_{TV}(V)$ represents the tension-velocity relationship. Except for the F_{max}, the other parameters are not specific to the modeled muscle and must be optimized through curve fitting.

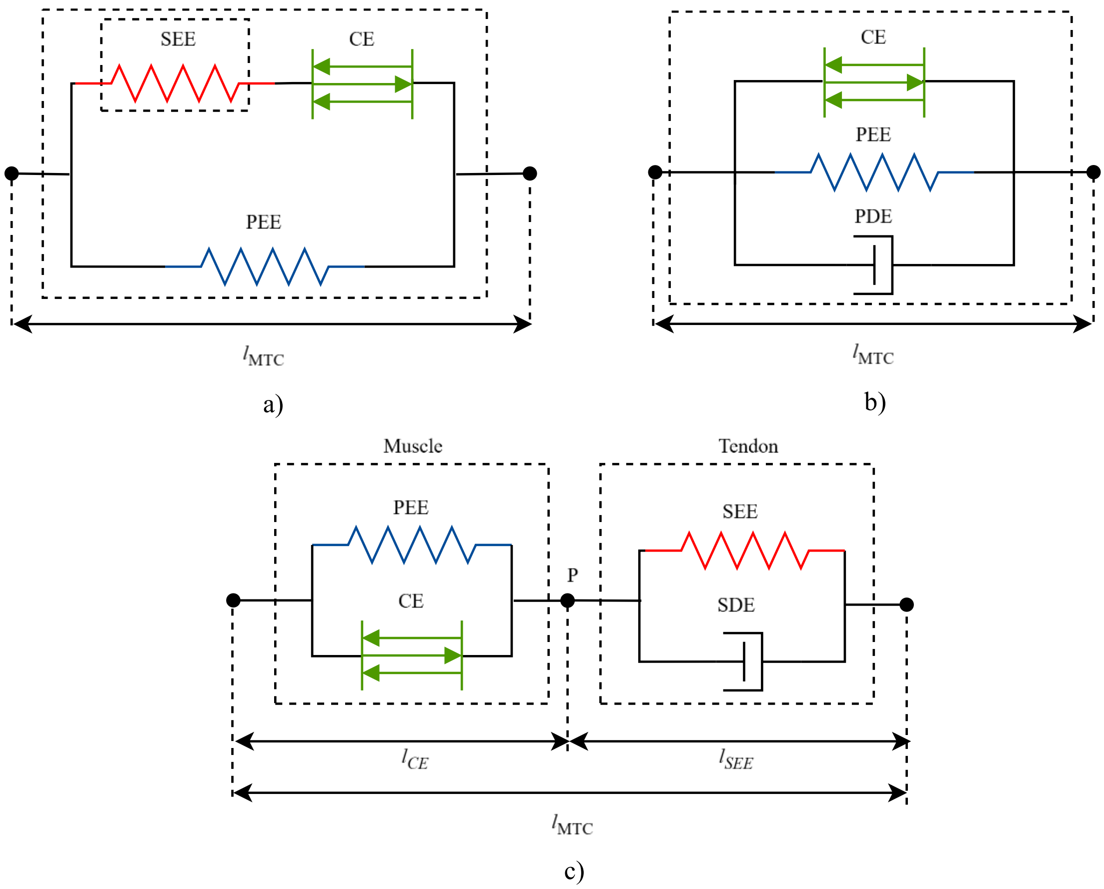

Figure 1. Schematic representation of a) *MAT_S15, b) *MAT_156 and c) EHTM internal structures

The EHTM model is an open-source material model designed to simulate a complete Muscle-Tendon Complex (MTC) [8]. In this model, the muscle and tendon are represented separately (Figure 1 c)). The muscle is defined by the CE and PEE element, whereas the tendon comprises the SEE element and, as an extension in the EHTM, the additional serial damping element (SDE) [9]. Unlike the `*MAT_156` and `*MAT_S15` models, the EHTM utilizes muscle-specific parameters, such as maximum isometric force and muscle length, along with non-specific parameters and constants found in the literature. The force in the EHTM is defined by the balance between the muscle and tendon unit and is expressed as follows:

$$Force_{Muscle} = Force_{Tendon} \qquad \text{(Equation 2)}$$

$$F_{CE}(l_{CE}, \dot{l}_{CE}, q) + F_{PEE}(l_{CE}) = F_{SEE}(l_{MTC}, l_{CE}) + F_{SDE}(l_{CE}, \dot{l}_{CE}, \dot{l}_{MTC}, q) \qquad \text{(Equation 3)}$$

where l_{CE} – is the length of the muscle, l_{SEE} is the length of the tendon, l_{MTC} – is the length of the MTC, defined as $l_{MTC} = l_{CE} + l_{SEE}$, $\dot{l}_{CE}$ – is the contraction velocity of the contractile element (CE), q – represents muscle activity.

Moreover, the EHTM internally computes muscle activation levels at runtime based on stimulation values from a controller, using various integrated activation dynamics methods, such as Hatze, modified Hatze, and Zajac, thereby eliminating the need to set predefined activation levels and perform curve fitting, as for `*MAT_156` [10]. The model includes an integrated PD controller with four strategies: an open-loop strategy, a closed-loop length feedback strategy, a hybrid controller, and a stretch reflex-based controller. These control loops are integrated into the Fortran user material subroutine and are executed with greater speed compared to standard LS-DYNA keyword declarations which are interpreted in runtime. These features make the EHTM a suitable candidate for AHBM development.

Development of a Hybrid Muscle Model

Hybrid muscle modeling is a technique that decomposes the stresses generated by a muscle model into those from a passive 3D structure and active truss elements. The concept of a Superpositioned Muscle Finite Element (SMFE) is shown in Figure 2. Its variant has previously been explored in [11], where one-dimensional active truss elements with a three-dimensional hyperelastic and viscoelastic passive matrix were integrated into one model. Besides, different combinations of **`*MAT_156`** and **`*MAT_SIMPLIFIED_RUBBER (*MAT_181)`** have been utilized to implement similar hybrid muscle approach AHBMs by other researchers [1, 12, 13].

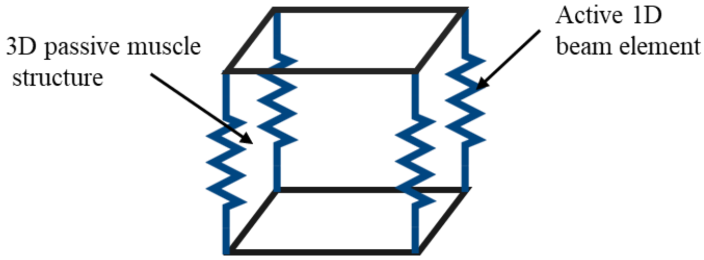

Figure 2. Schematic representation of a hybrid modelling technique.

An additive decomposition of the Cauchy stresses separates the active and passive components, resulting in the following relationship:

$$\sigma_{total} = \sigma_{passive} + \sigma_{active} \qquad \text{(Equation 4)}$$

where the $\sigma_{active} = {}^{F_{active}}/_{PCSA}$ with $PCSA$ being the physiological cross-section of the muscle, as available in the anatomical literature sources.

Hybrid Muscle Model Integration into Ansys Hans HBM

The muscles of the Ansys Hans [3] consist of distinct part components that represent the muscle tissue, a muscle transition zone (similar to an aponeurosis), and a tendon as seen in Figure 3. The proposed hybrid model has been integrated into the HBM by combining the EHTM model, which functions as 1D active elements, with the hyperelastic simplified rubber model (**`*MAT_181`**) used for the muscles. The active fibers extend throughout the entire length of the muscle tissue part and connect to the tendon. Each strand of fiber has a unique part ID and is modeled as **`*PART_AVERAGED`** [10], enabling the series of 1D elements to behave similarly to a single 1D element with muscle material model created using traditional meshing methods.

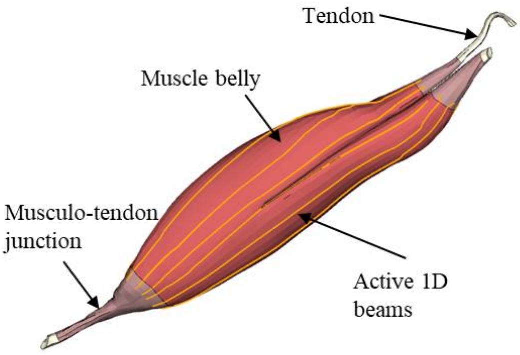

Figure 3. Isolated bicep brachii muscle with active 1D beam elements.

VALIDATION OF A HYBRID MUSCLE MODELLING APPROACH

The proposed modelling approach is validated at a system level in the following to ensure it can produce the correct forces and replicate the fundamental force-length relationship using experiments described in the literature.

Stress-Strain Relation

To validate the modelling method, the authors utilized experimental data from [14], in which the tibialis anterior (TA) muscle of a New Zealand white rabbit was elongated at three different strain rates: 1, 10, and 25 Hz. The passive 3D portion of the muscle was modeled using **`*ELEMENT_SOLID`** with **`*MAT_181`** and was fixed at one end in all degrees of freedom. The active part of the muscle was tested sequentially with different materials: the default **`*MAT_S15,`** the standard EHTM, and a modified EHTM. Prior to being stretched to achieve 25% of the initial strain, the muscle was fully activated using a Hatze activation dynamics curve in the simulation. A cross-section was taken at the midpoint of the muscle belly to measure stress (see Figure 4).

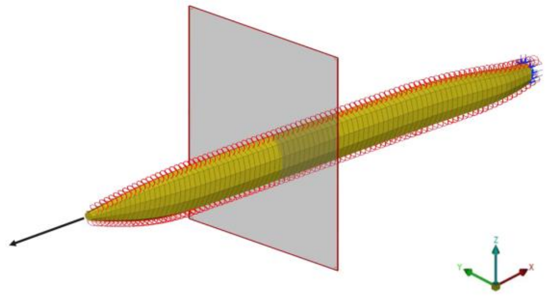

Figure 4. Boundary condition for the stress strain-validation simulation.

Force-Length Relationship

The isometric force-length relationship between CE length and the force it can produce was validated according to the protocol described in [1]. Unlike the **`*MAT_S15`**, which requires the force-length relationship to be input through curve fitting, the EHTM calculates this relation at runtime. By comparing the resulting curves, we can assess how accurately the EHTM predicts the corresponding forces. A test simulation was conducted with a constant muscle activation level of 0.3, during which the muscle was stretched to various lengths, and the resulting forces were plotted for each length.

<u>Stress-Strain Response of a Hybrid Muscle</u>

The stress developed in the muscle belly was compared against the different material models used to model the active beam elements and with the earlier studies shown in Figure 5. During the simulation runs, it became apparent that the default EHTM in a hybrid setting exhibited a very stiff response and poor correlation between experimental stress and strain. To address this issue, a modified version of the EHTM was introduced and tested. The modified EHTM is an extraction from the complete model that includes only the muscle part components (see Figure 1 c). Corresponding changes were made in the user material subroutine to reflect this adjustment.

Table 1 compares the normalized root mean square errors (NRMSE) of the different models with the experimental data sources. The results indicate that the modified EHTM has the lowest NRMSE. Comprehensive comparison between **`*MAT_S15`** and the modified EHTM reveals that **`*MAT_S15`** exhibits instability at higher strain rates, which leads to necking and uneven extension at high strains near the transition zone (see Figure 6.). In contrast, the modified EHTM demonstrates a stable response, making it an ideal choice for highly dynamic simulations, such as vehicle crashes.

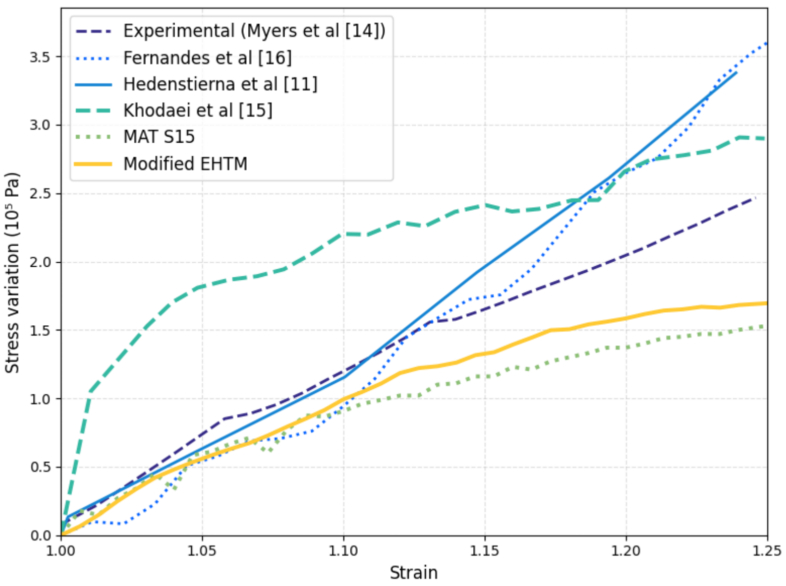

Figure 5. Stress variation for different material models used in hybrid setting.

Table 1.
Simulation setup vs NRMSE

Simulation setup	NRMSE
Khodaei et al. [15]	33%
Hedenstierna et al. [11]	20%
Fernandes et al. [16]	17%
MAT_S15	17%
Modified EHTM	15%

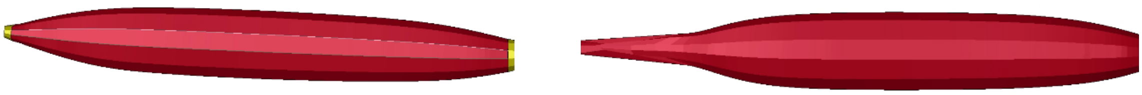

Figure 6. Final time step of the simulation with modified EHTM (left) and *MAT_S15 (right).

<u>Force-Length Relationships of a Hybrid Muscle</u>

The simulation of the isometric force-length relationship demonstrates a close correlation with the results in [1, 17] as seen in Figure 7. The normalized force-length curve indicates that the combination of **`*MAT_181`** and the modified EHTM successfully replicates the essential response of the Hill-type model. Additionally, the width and the exponential factor on both the ascending and descending limbs of the curve can be adjusted using specific parameters on the EHTM material card.

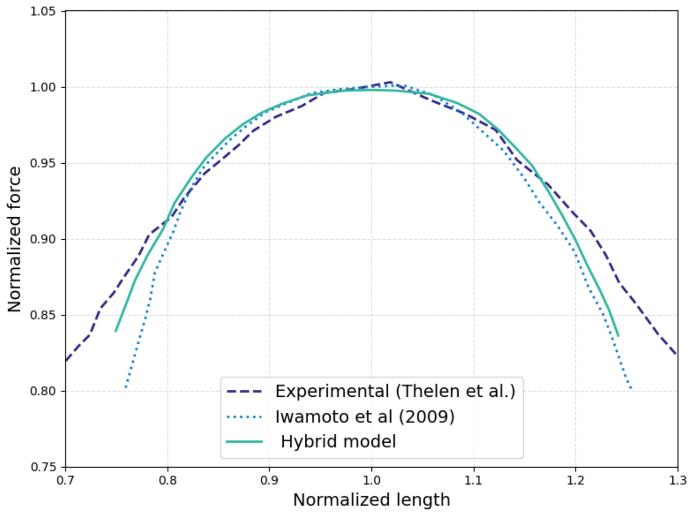

Figure 7. Force-length relationship.

SIMULATIONS WITH THE ANSYS HANS PEDESTRIAN HBM

To facilitate comparison of the two diverse muscle-modelling approaches, the EHTM and the hybrid muscle model were implemented within the Ansys Hans pedestrian model to model the kinematics of an active leg. The swing phase of the gait cycle was chosen for the study of the influence of modelling technique. In the traditional 1D modelling approach using EHTM, to accurately represent the leg's gait-cycle swing phase, nine essential muscles that play a significant role in this motion were modelled, as illustrated in Figure 8 (center). The nine muscles are as follows: Semitendinosus, Biceps femoris long head, Vastus medialis, Gastrocnemius medialis, Gastrocnemius lateralis, Tibialis anterior, and soleus. The origin, insertion, and routing points for the one-dimensional beam elements were derived from anatomical sources and correspond to the attachment points of the three-dimensional muscles in the Ansys Hans HBM Figure 8 (right).

To transfer the forces from one-dimensional muscles to the bones, the beam elements were connected to the muscles via **`*CONSTRAINED_NODAL_RIGID_BODY`** (NRBs). The routing points around the hip and the knee joint (including the patella), as well as the ankle are particularly crucial as they ensure precise transmission of the resulting joint moments. These routing points are nodes that are also linked to the bones through NRBs. They represent the muscle moment arms and thereby convert the axial muscle force into a rotational moment around the respective joint Figure 8 (left). The EHTM muscle-specific parameters were obtained from the study, where AHBM was developed by incorporating 658 controlled Hill-type EHTM muscles adapted from a scalable muscle-driven multibody HBM into the THUMS V4.02 AM50 Pedestrian [5], with further adaptation incorporating the activation levels reported in the experiment [19].

To enable a direct comparison with the conventional one-dimensional beam-element modeling approach, the same nine leg muscles were also modeled using the hybrid muscle modeling approach with modified EHTM. No additional one-dimensional beam elements or routing points were required, as the existing three-dimensional muscle geometries within the Ansys Hans model, along with the Macro Fiber Technology (MFT), were directly utilized for hybrid muscle modeling.

The upper body of the Ansys Hans HBM was initially positioned in a posture from the Euro NCAP pedestrian human model certification TB 024 protocol [18]. In contrast, the lower body was set with the right leg at an angle, ready to initiate the swing phase of a gait cycle shown in Figure 8 (left). The positioning was carried out using Oasys PRIMER Version 21.0 software with the knee angle $\varphi_K = 122°$ and the hip angle $\varphi_H = 161°$. The activation levels for the swing phase were obtained from the experiments of [19] given in Table 2. The hip was constrained in a fixed position across all degrees of freedom using the **`*BOUNDARY_SPC`** keyword.

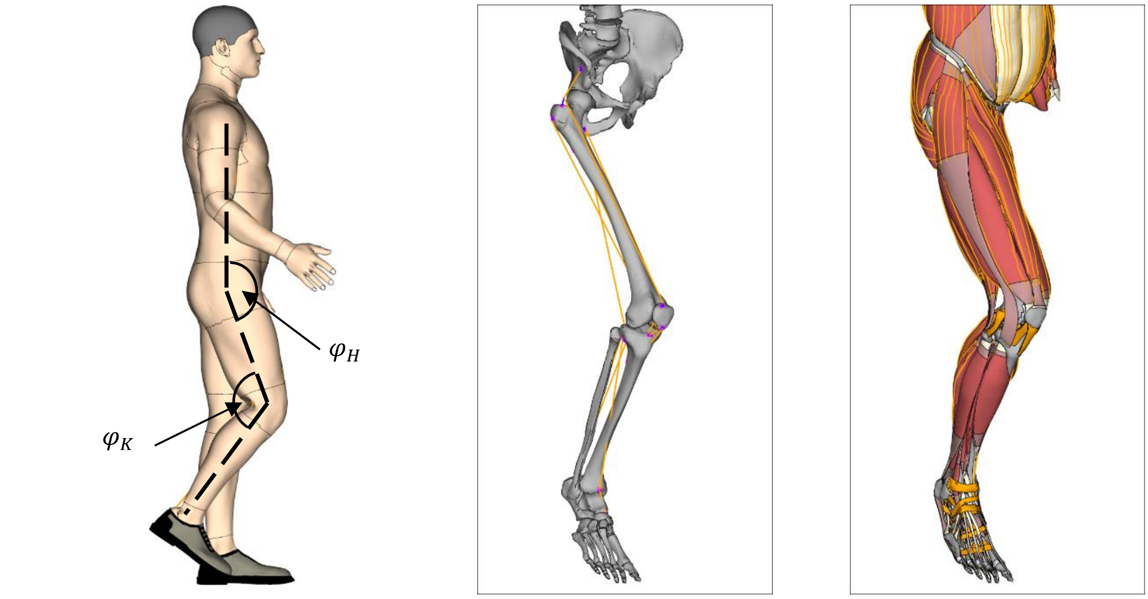

Figure 8. Angular System in the Hans Pedestrian Model (left), EHTM Muscle Routing in the leg (center) and Hybrid Muscle Modelling in the leg (right).

Table 2
Muscle activation levels – Swing phase

Muscle	Activation level
Semitendinosus	50 %
Bicep femoris long head	20 %
Rectus femoris	30 %
Vastus medialis	30 %
Gastrocnemius medialis	30%
Gastrocnemius lateralis	30 %
Tibialis anterior	60 %
Soleus	10 %

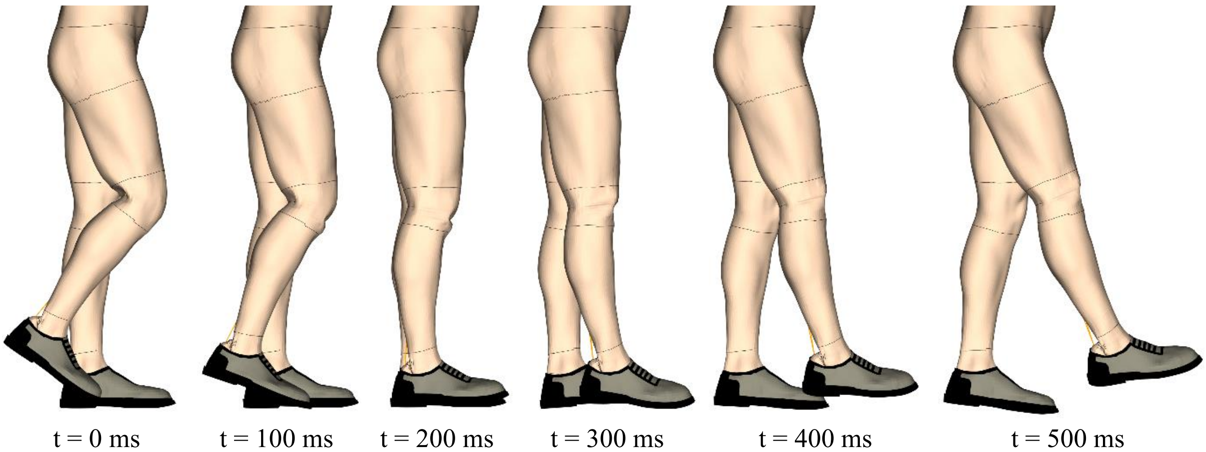

Figure 9. Gait cycle swing phase.

The simulations for both models ran for 500 ms and showed that, with the provided activation scheme, they successfully reproduced the swing phase shown in Figure 9. However, the hybrid model can achieve the final angles faster than the traditional 1D method, as seen from Figure 10.

Results from the gait cycle simulation were used to determine the initial positions for the impact study of an active pedestrian model with a family car (FCR) generic vehicle (GV), as specified in the Euro NCAP TB024 protocol. The impact time was defined as the time required for the particular model to reach the highest hip and knee angles. This would also ensure that the initial positions in both cases are identical and eliminate differences that can arise from positioning. For the hybrid model, the impact time was set to 150 ms, and for the EHTM model, it was set to 223 ms. At this time the knee and hip angles are approximately 177°. The models would be activated with the activation scheme from Table 2 until they reach the angles at the impact times, before being impacted by the FCR. The active simulations are also compared against a passive model that has a similar initial position at the time of impact.

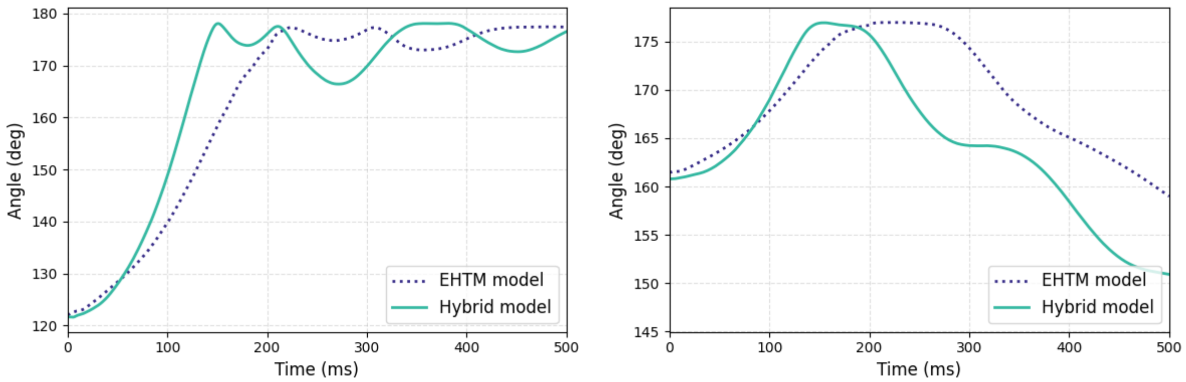

Figure 10. Angle variation over time for the knee (left) and hip (right) joints.

Results

The modelling methods are compared by evaluating differences in the global kinematics of HBM as well as the cross-sectional forces generated by the model when the muscles are activated. The curves have been shifted to start at the time of impact, eliminating any time shifts that would otherwise arise from different impact times.

The nodal trajectories of the model are measured at the following points (Figure 11): HC – head center of gravity (COG), C7 – 7th vertebra in the cervical spine, T12 – 12th vertebra in the thoracic spine, AC – acetabulum center, KR – right knee joint, and AR – right ankle joint as seen from Figure 11. The forces are measured at the cross-sections (CRS) of the femur and the lower leg.

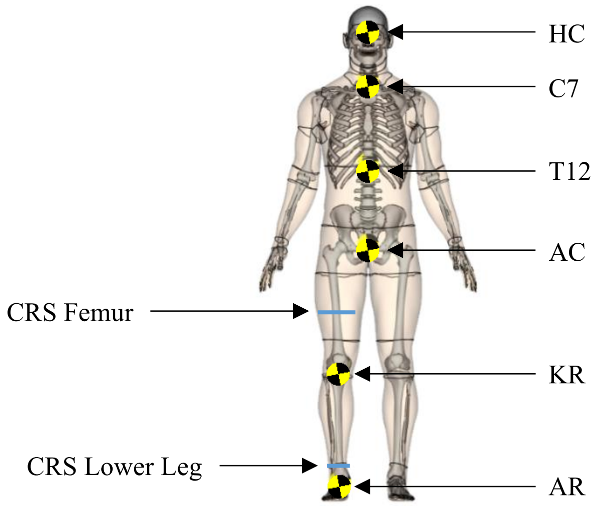

Figure 11. History nodes and cross-sections for the evaluation.

Kinematic response

The resulting kinematics of the body reveal that the impact point on the HBM's head is on the bonnet across all modelling approaches at an impact speed of 20 km/h (see Figure 12). The passive model and the one with the hybrid muscle model exhibit similar responses, differing only in body rotation. The head impact point of the passive model is more on the posterior side compared to the lateral side in the case of the hybrid model (see Appendix 1). This leads to a shorter head impact time in the passive model, with the acceleration of the head COG being 18% higher (0.51 mm/ms²) than in the active model (0.43 mm/ms²) (Figure 13 left).

The EHTM model demonstrates an entirely different response. Due to the one-dimensional beam elements routing around the knee joint and its connections to the patella, they aim to maintain the shortest distance to minimize forces and keep the MTC in equilibrium. Therefore, at the time of impact, the patella is displaced out of the joint and attempts to maintain this position to keep the joint forces in equilibrium. This results in an unnatural response, with the lower leg pulled along the Z-axis of the bumper rather than exhibiting pendulum-like motion (AR curve – Figure 12). Consequently, the upper-body kinematics is also influenced, resulting in a shorter head impact time and an increased head COG acceleration of 77.6 mm/ms².

The Head Injury Criterion (HIC15) [20] values obtained in the simulations for the different modeling approaches are as follows: Hybrid – 120.7, EHTM – 216.8, and Passive – 160.7. These values indicate a low probability of severe head injury according to the Abbreviated Injury Scale (AIS).

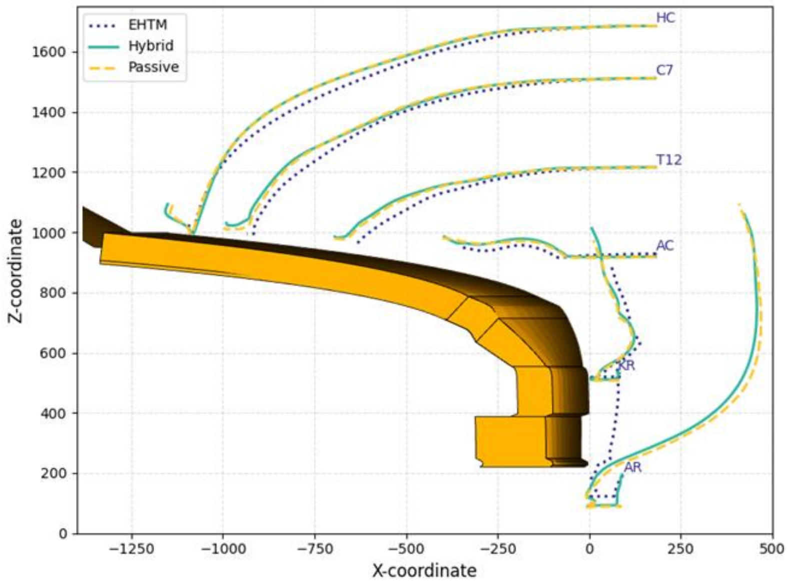

Figure 12. Trajectories of landmark points at 20 km/h impact velocity.

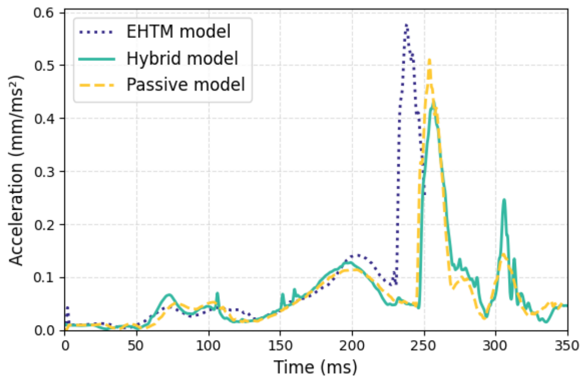

Figure 13. Head COG acceleration at 20 km/h.

<u>Cross-sectional forces:</u>

The cross-sectional forces at the mid-section of the femur and the lower part of the leg point of impact at the leading edge (see Figure 11 for positions) are measured across various models for 20 km/h and are demonstrated in Figure 14. It was observed that the hybrid model exhibited lower forces in both sections. This finding is consistent with the argument that the activated muscle is stiffer, resulting in less force being transmitted to the bones.

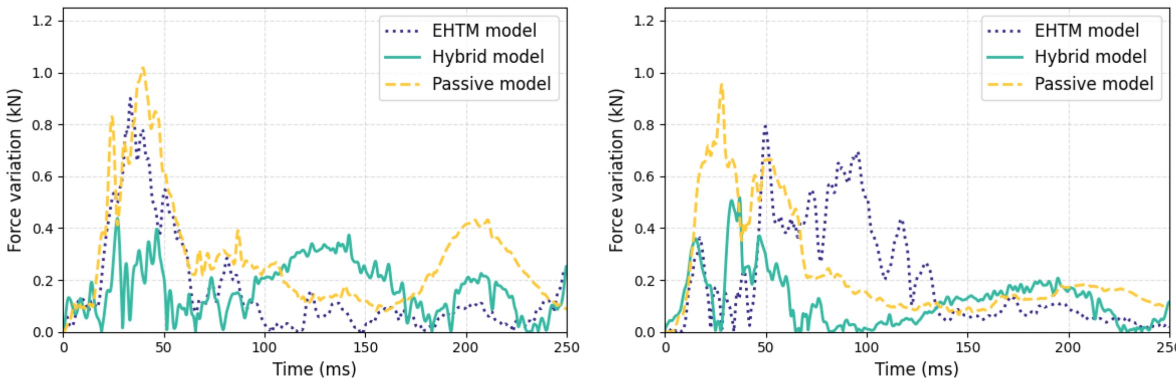

Figure 14. Force variation at 20 km/h in the cross-section of the Femur bone (left) and the lower leg (right).

DISCUSSION

This contribution explores a method for modeling active muscles in HBM using one-dimensional active beam elements combined with three-dimensional passive solid elements into a hybrid structure. The simulation of the activated lower body during a pedestrian impact scenario demonstrates that this hybrid muscle-activation strategy affects kinematics and force distribution. In addition, the results indicate that the muscle routing in the one-dimensional traditional approach also affects these factors. While the traditional modeling approach is optimized to generate movements for specific ranges of motion, vehicle impact scenarios are highly dynamic and require a more robust solution. By leveraging the underlying three-dimensional structure of the muscles and connective tissue, proposed hybrid modelling method can address these limitations. Moreover, the lower-body kinematics showed considerable improvement and stability when using a hybrid muscle structure. Due to the low impact velocity, none of the elements exceeded a Maximum Principal Strain of 1.5 % in the cortical bones of the legs [21], which means no fractures were predicted.

Another advantage of using the hybrid model is the effective distribution of forces at the points of origin and insertion of the muscle belly. In the model where 1D EHTM beams are attached to the bones using NRBs, stress concentrations and localized deformations on the cortical bone were documented. These factors can further impact the transmission of forces across various joints. This finding directly correlates with the results of the gait cycle swing-phase simulation, in which the hybrid model achieved the target angles more quickly than the conventional approach.

This study did not account for upper-body muscle activation, which may have influenced spinal and neck stiffness and contributed to the observed values. Recent studies employing AHBMs with simplified 1D muscle representations have shown that muscle activation levels and timing in the upper body significantly affect not only occupant response in frontal, lateral, and rear impacts, but also pedestrian behaviour in collisions with vehicles. As a result, findings in the current contribution may not accurately reflect the actual injury mechanics encountered in real-world scenarios. Detailed validation using the accident reconstruction method could provide greater clarity on this point.

CONCLUSIONS

The proposed method improves existing computational HBMs by accurately representing physiological muscle structures. This enhancement allows for better modeling of both active and reactive human responses. While the method demonstrates explicit advantages over traditional approaches, it has been tested only on an isolated pedestrian impact load case, focusing on the muscle activation of one leg impacting a generic family car model. The authors intend to broaden the study in the future to include various vehicle types, as these can significantly affect kinematics and injury responses. Additionally, the modeling of active muscles should expand beyond the extremities to include the upper body. Currently, the setup utilizes an open-loop muscle controller that relies on predefined activation values. Improved models will aim to employ the controller within the EHTM model to dynamically compute muscle activation values during simulation runtime. This development will facilitate the simulation of active pedestrian responses both before and during an impact.

ACKNOWLEDGEMENTS

This conference paper was written as part of the project "CARpulse: Capsule for autonomous vehicle platforms for safe individual transport in all areas of life", funded by the Federal Ministry of Education and Research (BMBF) under the funding code 02P23Q800 as part of the "Research Campus – Public-Private Partnership for Innovation" funding initiative, and supervised by the Project Management Agency Karlsruhe (PTKA). The authors would like to thank Tobias Erhart for sharing his valuable knowledge in LS-DYNA User Interfaces and helpful advice. The consortium partners would like to thank BMBF for the funding provided and PTKA for its support.The responsibility for the content of this publication lies with the authors.

REFERENCES

[1] Iwamoto, M., Nakahira, Y., Kimpara, H., & Sugiyama, T. (2009). Development of a Human FE Model with 3-D Geometry of Muscles and Lateral Impact Analysis for the Arm with Muscle Activity. In SAE Technical Paper Series (Vol. 1). Digital Human Modeling for Design and Engineering Conference and Exhibition. SAE International. https://doi.org/10.4271/2009-01-2266

[2] Gayzik, F. S., Moreno, D. P., Vavalle, N. A., Rhyne, A. C., & Stitzel, J. D., Development of a Full Human Body Finite Element Model for Blunt Injury Prediction Utilizing a Multi-Modality Medical Imaging Protocol, In 12th International LS-DYNA Users Conference, 2012, Detroit, USA.

[3] Gromer, A., Fressmann, D., Johansen, T., Mandel, S., Högberg, L., Sible, S.,The Ansys Human Body Model Ecosystem Presentation at 2025 EMEA Ansys Transportation Summit and International LS-DYNA Conference, Oktober 2025.

[4] Trube, N., Riedel, W., & Boljen, M. (2021). How Muscle Stiffness Affects Human Body Model Behavior. BioMedical Engineering OnLine, 20(1). https://doi.org/10.1186/s12938-021-00876-6

[5] Trube, N., Lerge, P., Nölle, L. V., Mönnich, J., Lich, T., & Schmitt, S. (2024). Development and Plausibility Assessment of an Active Human Body Model in Numerical Cyclist-to-Vehicle Collision Simulations Based on Real-Life Accident Data. In Conference proceedings of the International Research Council on the Biomechanics of Injury (IRCOBI), Stockholm, Sweden. https://www.ircobi.org/wordpress/downloads/irc24/pdf-files/2479.pdf

[6] Hill, A.V. (1938). The Heat of Shortening and the Dynamic Constants of Muscle. Proceedings of the Royal Society of London. Series B, 126, 136–195. https://doi.org/10.1098/rspb.1938.0050

[7] ANSYS, Inc. (2025). LS-DYNA Keyword User's Manual: Volume II – Material models (R16). https://lsdyna.ansys.com/wp-content/uploads/2025/04/LS-DYNA_Manual_Vol_II_R16.pdf

[8] Kleinbach, C., Martynenko, O., Promies, J., Haeufle, D. F. B., Fehr, J., & Schmitt, S. (2017). Implementation and Validation of the Extended Hill-Type Muscle Model with Robust Routing Capabilities in LS-DYNA for Active Human Body Models. BioMedical Engineering OnLine, 16(1). https://doi.org/10.1186/s12938-017-0399-7

[9] Günther, M., Schmitt, S., & Wank, V. (2007). High-Frequency Oscillations as a Consequence of Neglected Serial Damping in Hill-Type Muscle Models. Biological Cybernetics, 97(1), 63–79. https://doi.org/10.1007/s00422-007-0160-6

[10] Martynenko, O. V., Kempter, F., Kleinbach, C., Nölle, L. V., Lerge, P., Schmitt, S., & Fehr, J. (2023). Development and Verification of a Physiologically Motivated Internal Controller for the Open-Source Extended Hill-Type Muscle Model in LS-DYNA. Biomechanics and Modeling in Mechanobiology, 22(6), 2003–2032. https://doi.org/10.1007/s10237-023-01748-9

[11] Hedenstierna, S., Halldin, P., & Brolin, K. (2008). Evaluation of a Combination of Continuum and Truss Finite Elements in a Model of Passive and Active Muscle Tissue. Computer Methods in Biomechanics and Biomedical Engineering, 11(6), 627–639. https://doi.org/10.1080/17474230802312516

[12] Putra, I. P. A., Carmai, J., Koetniyom, S., & Markert, B. (2015). The Effect of Active Muscle Contraction on Pedestrian Kinematics and Injury During Vehicle–Pedestrian Collision. In 10th European LS-DYNA Conference 2015, Würzburg, Germany.

[13] Mo, F., Li, J., Dan, M., Liu, T., & Behr, M. (2019). Implementation of Controlling Strategy in a Biomechanical Lower Limb Model with Active Muscles for Coupling Multibody Dynamics and Finite Element Analysis. Journal of Biomechanics, 91, 51–60. https://doi.org/10.1016/j.jbiomech.2019.05.001

[14] Myers, B. S., Woolley, C. T., Slotter, T. L., Garrett, W. E., & Best, T. M. (1998). The Influence of Strain Rate on the Passive and Stimulated Engineering Stress–Large Strain Behavior of the Rabbit Tibialis Anterior Muscle. Journal of Biomechanical Engineering, 120(1), 126–132. https://doi.org/10.1115/1.2834292

[15] Khodaei, H., Mostofizadeh, S., Brolin, K., Johansson, H., & Östh, J. (2013). Simulation of Active Skeletal Muscle Tissue With a Transversely Isotropic Viscohyperelastic Continuum Material Model. Proceedings of the Institution of Mechanical Engineers, Part H: Journal of Engineering in Medicine, 227(5), 571–580. https://doi.org/10.1177/0954411913476640

[16] Fernandes, N. A. T. C., Schmitt, S., & Martynenko, O. V. (2019). Modelling and Validation of the 3D Muscle–Tendon Unit with Solid Finite Elements in LS-DYNA for Active Human Body Model Applications. In Conference proceedings of the International Research Council on the Biomechanics of Injury (IRCOBI), Florence, Italy. http://www.ircobi.org/wordpress/downloads/irc19/pdf-files/47.pdf

[17] Thelen, D. G. (2003). Adjustment of Muscle Mechanics Model Parameters to Simulate Dynamic Contractions in Older Adults. Journal of Biomechanical Engineering, 125(1), 70–77. https://doi.org/10.1115/1.1531112

[18] Klug, C., Feist, F., Schneider, B., Sinz, W., Ellway, J., & van Ratingen, M. (2019). Development of a Certification Procedure for Numerical Pedestrian Models. In Proceedings of the 26th International Technical Conference on the Enhanced Safety of Vehicles (ESV) (pp. 1–24). Eindhoven, Netherlands. https://www-nrd.nhtsa.dot.gov/pdf/ESV/Proceedings/26/26ESV-000310.pdf

[19] Barrett, R. S., Besier, T. F., Lloyd, D. G. (2007). Individual muscle contributions to the swing phase of gait: An EMG-based forward dynamics modelling approach. Simulation Modelling Practice and Theory 15(9), 1146–1155. https://doi.org/10.1016/j.simpat.2007.07.005

[20] Versace, J., "A Review of the Severity Index," SAE Technical Paper 710881, 1971, https://doi.org/10.4271/710881.

[21] Wu, T., Kim, T., Bollapragada, V., Poulard, D., Chen, H., Panzer, M. B., Forman, J. L., Crandall, J. R., & Pipkorn, B. (2017). Evaluation of biofidelity of THUMS pedestrian model under a whole-body impact conditions with a generic sedan buck. Traffic injury prevention, 18(sup1), S148–S154. https://doi.org/10.1080/15389588.2017.1318435

APPENDIX-1

FCR impact kinematics at 20 km/h

Time (ms)	Passive model	EHTM model	Hybrid model
0 ms	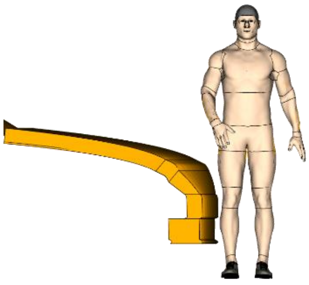	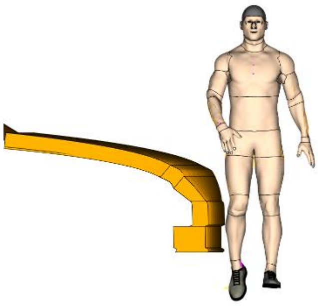	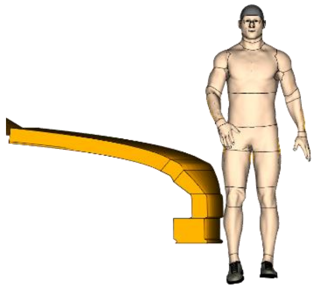
100	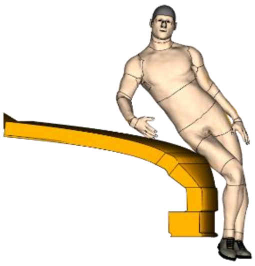	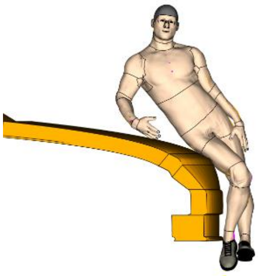	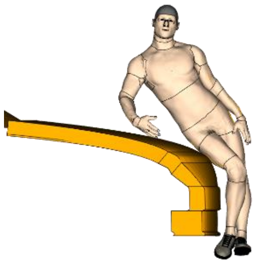
200	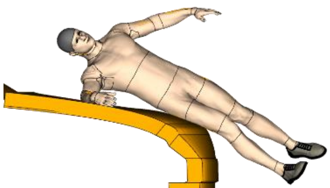	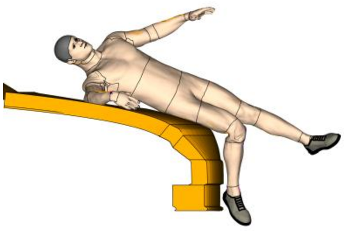	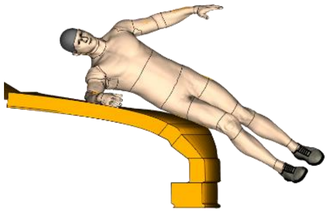
250